

Submitted: 2024-08-01 | Revised: 2024-09-07 | Accepted: 2024-09-22

Keywords: Sentinel-3, algal bloom, remote sensing, chlorophyll-a, semantic segmentation, rule-based classifier

Venkatesh BHANDAGE [0000-0002-9503-8196]*,
Manohara PAI M. M. [0000-0003-2164-2945]**

SEMANTIC SEGMENTATION OF ALGAL BLOOMS ON THE OCEAN SURFACE USING SENTINEL 3 CHL_NN BAND IMAGERY

Abstract

Satellite imagery plays an important role in detecting algal blooms because of its ability to cover larger geographical regions. Excess growth of Sea surface algae, characterized by the presence of Chlorophyll-a (Chl-a), is considered to be harmful. The detection of algal growth at an earlier stage may prevent hazardous effects on the aquatic environment. Semantic segmentation of algal blooms is helpful in the quantization of algal blooms. A rule-based semantic segmentation approach for the segregation of sea surface algal blooms is proposed. Bloom concentrations are classified into three different concentrations, namely, low, medium, and high. The chl_nn band in the Sentinel-3 satellite images is used for experimentation. The chl_nn band has exclusive details of the presence of chlorophyll concentrations. A dataset is proposed for the semantic segmentation of algal blooms. The devised rule-based semantic segmentation approach has produced an average accuracy of 98%. A set of 100 images is randomly selected for testing. The tests are repeated on 5 different image sets. The results are validated by the pixel comparison method. The proposed work is compared with other relevant works. The Arabian Sea near the coastal districts of Udupi and Mangaluru has been considered as the area of study. The methodology can be adapted to monitor the life cycle of blooms and their hazardous effects on aquatic life.

1. INTRODUCTION

Algal bloom on the sea surface is caused by the excessive and uncontrolled growth of algae. They grow excessively under typical environmental conditions such as eutrophication. They produce harmful effects on the environment, such as marine water contamination and a large number of fish deaths. With their bulk presence, they can impact the economy (Ho et al., 2019) and even cause a huge number of fish deaths (Fogg, 2022; Roelke et al., 2001).

* Manipal Academy of Higher Education, Manipal Institute of Technology, Department of Computer Science and Engineering, Manipal 576104, Karnataka, India, venkatesh.bhandage@manipal.edu

** Manipal Academy of Higher Education, Manipal Institute of Technology, Department of Information and Communication Technology, Manipal 576104, Karnataka, India, mmm.pai@manipal.edu

Hence, there is a need to subside the excessive growth of algal blooms at an earlier stage. Algal blooms can be predicted, detected, and monitored using various approaches, such as the usage of chlorophyll-a and phycocyanin proxies, as in Fernández-Tejedor et al. (2022), Ogashawara (2019), Vase et al. (2022), Kutser (2009) and Randolph et al. (2008). Image processing finds different applications in areas such as expression analysis (Kinane Daouadji & Bendella, 2024), hand gesture recognition (Elbahri et al., 2024), breast cancer detection (Al-Nawashi et al., 2024), human stress detection (Baran, 2024), copyright protection (Makhlouf et al., 2024), and classifying the type of soil (Maiyanti et al., 2023). Similarly, image processing can also be adopted in the study of algal blooms. Imagery captured by sensors on board satellites and unmanned aerial vehicles (UAVs) can be used for algal bloom studies (Haji Gholizadeh et al., 2016). The satellite images are predominantly used in monitoring and studying algal blooms, as evident in research by Cui et al. (2022), Zhu et al. (2023), Ogashawara (2019), Rodríguez-Benito et al. (2020), and Nayak et al. (2023). Sentinel 3A/3B images have different bands that can be used in various earth observation applications. One of the useful bands that is present in Sentinel 3A/3B products is the chl_nn band, which has exclusive information about the chlorophyll concentration in the region captured by the satellite. This band can be explored to study the algal bloom dynamics on the sea surface areas.

Semantic segmentation (Badrinarayanan et al., 2017) is the mechanism of assigning each and every pixel of an image to a specific class depending on the application. Semantic segmentation has been used in mapping different land cover areas (Kotaridis et al., 2022; Lilay & Taye, 2023; Singh et al., 2023), to classify crops and weeds (Radhika et al., 2022), to study the river dynamics from SAR images (Verma et al., 2021; Ravishankar et al., 2022), and to classify different regions from images captured using UAVs (Girisha et al., 2021a). The semantic segmentation technique has been least used for categorization of algal blooms into different concentrations. The categorization of algal blooms into different regions based on the chlorophyll content can help us study the impact of algal blooms on aquatic life and the economy. The Sentinel's Application Platform (SNAP) tool is effectively used to study the sentinel satellite imagery (Zhu et al., 2023). Figure 1 depicts the images of the Arabian Sea region, which is considered the study area in this research. The RGB image is obtained by using the band combination tool available in SNAP. Figure 1(a) shows the study area, specifically the square region within the image, as viewed by the World View option available in the SNAP tool. Figure 1(b) shows the corresponding RGB image.

Objectives of the research are:

1. To create a dataset for the algal bloom study.
2. To devise methodology for the semantic segmentation of algal blooms.

Main contributions of this research are:

1. Dataset of Sentinel 3A/3B chl_nn band images is created.
2. A rule-based approach for semantic segmentation of algal blooms is devised.

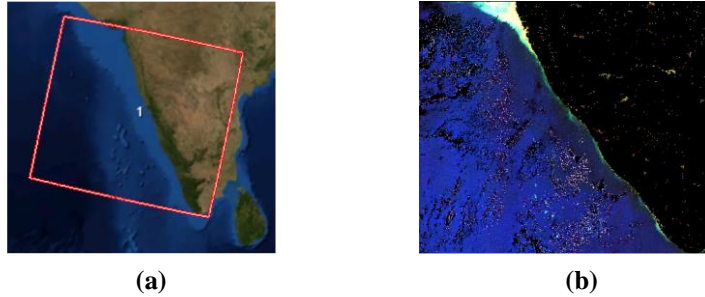


Fig. 1. Study area of Arabian sea being considered in this research (a) Study area as being seen by world view option available in SNAP tool (b) RGB Image obtained using default band combinations

This research is intended to develop a rule-based approach for semantic segmentation of sea surface algal blooms. A detailed review of the current state-of-the-art in the area of algal bloom detection and usage of semantic segmentation techniques is given in Section 2. Proposed methodology is presented in Section 3. Results and discussion are presented in section 4. Section 5 gives the conclusions.

2. LITERATURE SURVEY

To know the state of the art in the area of algal bloom detection, monitoring, and adoption of semantic segmentation for their study, a literature survey is carried out. The gist of the survey carried out is as below.

Fernández-Tejedor et al. (2022) have developed an algorithm for estimating the concentration of chlorophyll-A in the coastal area of the northwestern Mediterranean called the Ebro Delta. They have adopted various reflectance bands of atmospherically corrected Sentinel-2 images. Badrinarayanan et al. (2017) have presented a fully convolutional neural network (FCN) architecture for pixel-wise semantic segmentation called SegNet. The model is composed of an encoder, decoder, and pixel-wise classification layer. They have worked on road and indoor scene segmentation. Binge Cui et al. (2022) have proposed a method for extraction of green tides from Moderate-Resolution Imaging Spectroradiometer (MODIS) satellite images. They have adopted super-resolution technology with a deep semantic segmentation network (Se-Net). They have compared the performance of the proposed methodology with existing methods of green tide extraction. They have considered support vector machines (SVM), classification and regression trees (CART), random forest algorithms (RM), SegNet, and U-Net for comparison. Wang et al. (2023) have proposed a semantic segmentation network that uses hidden features from remote sensing images. The network produces accurate results of semantic segmentation by hierarchically fetching and combining feature information. They have experimented with the proposed network with the 15-Class Gaofen Image dataset and the ISPRS dataset.

Evan Shelhamer et al. (2017) have shown that convolutional neural networks can produce improved results in semantic segmentation when trained end-to-end and pixels-to-pixels on whole images. They have adapted GoogleNet, VGGNet, and AlexNet into convolutional networks for the task of segmentation. Yang and Tang (2021) have utilized geospatial hash codes with deep learning techniques for semantic segmentation of satellite images. Ma et al.

(2023) have proposed a deep learning architecture for analyzing scenes of Remote Sensing Images (RSIs). They have used multiscale adjacency information and multimodal fusion features. Ronneberger et al. (2015) have presented a variant of convolutional network called U-Net for semantic segmentation. The network can be trained with the help of a small number of images and image augmentation techniques. Radhika Kamath et al. (2022) have presented a semantic segmentation-based technique for classification of crops and weeds in a paddy field. They have used UNet, Pyramid Scene Parsing Network (PSPNet), and SegNet models. They have used Intersection over Union (IoU) for the measurement of the obtained classification results. Kotaridis Ioannis & Lazaridou Maria (2022) have presented an U-Net-based semantic segmentation approach. They have mapped different land cover areas, such as water, barren land, vegetation, and built-up. They have experimented with different combinations of spectral bands provided by Sentinel-2 imagery.

Lilay and Taye (2023) have presented a machine learning and deep learning-based semantic segmentation approach for land cover classification. They have used Sentinel-2 satellite images of their study area. Ningthoujam and Kishorjit (2023) have presented a Deep-Unet architecture for classification of different land fill areas. They have performed semantic segmentation on satellite images. They have used intersection over union (IoU) and global accuracy measures for evaluating the results produced by developed convolutional models. Zhu et al. (2023) have used U-net for identification of algal blooms from the combination of Sentinel-2A and Sentinel-2B satellite images. They have used ENVI 5.3 and SNAP 6.0 tools for the analysis. They have utilized combinations of different spectral bands to explore the algal bloom content in the image. Ogashawara (2019) has attempted to show that Sentinel-3 satellite images can be used effectively for mapping of cyanobacterial harmful algal blooms (CHABs). He used the optical characteristics of chlorophyll-a (chl-a) and phycocyanin (PC) pigments to explore the algal bloom concentration. Tendolkar et al. (2021) have presented an agrocopter to monitor the crop health. They have utilized the combination of semantic segmentation and the Normalized Difference Vegetation Index (NDVI) for identifying the class of crop as unhealthy, moderately healthy, and healthy. Ujjwal Verma et al. (2021) have presented an approach to measure the width of the river from synthetic aperture radar (SAR) images. They have adopted the technique of semantic segmentation with the help of deep learning models such as DeepLabV3+ and U-Net. The proposed methodology can be utilized for effective management of water resources across the coastal region.

Girisha et al. (2021b) have presented a UVID-Net for performing semantic segmentation of videos captured by using Unmanned Aerial Vehicle (UAV). They have performed transfer learning of U-Net on ManipalUAVid dataset for predicting four classes, such as water, construction, roads, and greenery. Girisha et al. (2021b) have proposed a conditional random field (CRF) framework for semantic segmentation of aerial videos with the help of temporal information. The proposed algorithm is experimented on ManipalUAVid dataset. The performance is evaluated with the help of mean intersection over union (mIoU). Li and Demir (2023) have used a modified version of U-Net architecture for extraction of water areas from Sentinel-1 images. They have used the open-access cloud platform Google Earth Engine (GEE) for collecting and preprocessing images. Tejas R. et al. (2022) have presented a modified U-Net-based approach for segmentation of rivers from the SAR images. They have adopted image inversion, thresholding, gamma correction, and multi-stage loss functions to improve the performance of segmentation tasks. Anilkumar and Venugopal

(2022) have presented a comprehensive review about the usage of deep learning-based techniques for semantic segmentation of satellite imagery. The survey addresses research gaps, recent advancements, and challenges in semantic segmentation. There exists a gap in the adoption of semantic segmentation for identification and classification of algal blooms. Rodríguez-Benito et al. (2020) have presented a study on advantages of using Sentinel-3 and Sentinel-2 images for algal bloom monitoring. They have presented the temporal, spatial, and spectral capabilities of these images for effective algal bloom observation.

Tholkapiyan et al. (2014) have used time series data of the Ocean Surface Algal Bloom Index (OSABI) for monitoring algal blooms on the Indian ocean surface. They have studied the geographical locations, extent of coverage, intensity of occurrence and interannual and seasonal variabilities of algal blooms. Nayak et al. (2023) have presented a comprehensive study on the spatial-temporal changeability of Chl-a across various biogeographic regions in the North Indian Ocean (NIO). They have considered images from the Ocean Color Monitor 2 (OCM2), MODIS, and Sea-Viewing Wide Field-of-View Sensor (SeaWiFS). Vinaya Kumar Vase et al. (2022) have validated the capabilities of satellite-based sensors to provide the Chl-a information present on the ocean surface. They have performed the comparison with sea truth data gathered from 204 stations across 3 years from 2015-2017. They have considered data from MODIS, Visible Infrared Imaging Radiometer Suite (VIIRS), and OCM2 sensors. They have found that OCM2 sensor data gives better results. Srichandan et al. (2022) have presented a study on the spatial and temporal distribution of phytoplankton blooms in the coastal regions of the Bay of Bengal (BoB). Jaiganesh et al. (2021) have presented a satellite-based approach to study the overall ocean productivity with the help of wind flow information, sea surface temperature (SST), and chlorophyll concentration datasets. Nallapareddy et al. (2022) have utilized Landsat-8 infrared images for classification of vegetation areas.

From the survey, it is evident that researchers have used Sentinel-2 images for algal bloom studies. The semantic segmentation technique is adopted for classification of different land cover fills and scene analysis. Little research is carried out on usage of the chl_nn band of Sentinel-3 images for semantic segmentation of algal blooms. There is no attempt made to develop a rule-based technique for semantic segmentation of algal blooms. Hence the research is carried out in the direction of semantic segmentation of Sentinel-3 images, specifically with the help of chl_nn band and rule-based technique.

3. PROPOSED METHODOLOGY

The dataset for algal bloom detection was created as there was no standard dataset. Sentinel 3 (S3) is a two-satellite mission comprising of Sentinel-3A (S3A) and Sentinel-3B (S3B). The data from both collections is available as open access to all the users. The Ocean and Land Color Instrument (OLCI) onboard S3 is an imaging spectrometer having a medium spatial resolution of 300 meters and 14-bit radiometric resolution. It provides 21 image bands with a temporal resolution of 1 day when combinations of S3A and S3B are considered together. For the purpose of our study, we have downloaded OLCI Level-2 Water Full Resolution (OL_2_WFR) products (EUMETSAT, 2024). A total of 23 images are considered in this research. Table 1 gives the details of some of the images used in this research. The life span of algal bloom varies from a few days to several months based on

environmental factors and seasonal conditions. We are attempting to segment the bloom concentrations within the given chl_nn band image. To make sure that our dataset has bloom concentrations of all the ranges, we have considered images in around 3 months. The images that have significantly less cloud coverage are identified and used. The combination of Sentinel-3A and Sentinel-3B images is used in this research to accommodate the increased revisit time of the geographical area being considered. The images captured by Sentinel-3A and Sentinel-3B satellites are identified by the prefixes S3A and S3B, respectively. The advantage of using sentinel products is that they provide temporal resolution of 1 day, which helps in continuous monitoring of blooms. They measure systematically Earth’s land, ice, oceans, and atmosphere to provide essential information in near-real time for weather forecasting. The disadvantage of these products is that they have a spatial resolution of 300 meters, which is not suitable to study smaller geographical areas.

Tab. 1. Details of some of the satellite imagery used in the research

| Acquisition date (dd/mm/yyyy) | Image |
|-------------------------------|--|
| 21/12/2021 | S3B_OL_2_WFR_20211221T050947_20211221T051247 |
| 29/12/2021 | S3B_OL_2_WFR_20211229T050218_20211229T050518 |
| 02/01/2022 | S3B_OL_2_WFR_20220102T045833_20220102T050133 |
| 30/01/2022 | S3A_OL_2_WFR_20220130T051149_20220130T051449 |
| 22/02/2022 | S3A_OL_2_WFR_20220222T051531_20220222T051831 |
| 26/02/2022 | S3A_OL_2_WFR_20220226T051146_20220226T051446 |
| 28/02/2022 | S3B_OL_2_WFR_20220228T052059_20220228T052359 |
| 01/03/2022 | S3B_OL_2_WFR_20220301T045448_20220301T045748 |

3.1. Dataset creation

The Sentinel’s Application Platform 9.0.0 (SNAP 9.0.0), an open source product, is utilized for analysis of Sentinel 3 products. Sentinel 3 satellite images have a specific band called CHL_NN, which explores the presence of chlorophyll in the satellite images. Upon opening the band in the explorer, we will be able to see the default grayscale image of the region being covered by the satellite imagery, as shown in Fig. 2. At the bottom left corner of the figure is the area of the Arabian Sea being considered for analysis. The corresponding image of the CHL_NN band is displayed at the right portion of the figure. Every pixel of this image has the information of its longitude and latitude, along with the amount of chlorophyll contained in it. This image can be exported for further analysis.

SNAP has built-in palettes for exploring the visual representations of the satellite images. These palettes are helpful in assigning the individual pixels of the image to different groups based on the value of chlorophyll present in them. SNAP has the provision to explore the images either by using the range of chlorophyll values present in the CHL_NN band image or by using the values present in the color palette definition. The range of chlorophyll value may differ from one satellite image to another. We can define our own color palette definition file, and we can have a maximum of 256 color definitions. Once the color palette is defined, it can be adopted for analyzing all the images in the same way. Hence, we have considered exploring or visualizing all the CHL_NN band images by using palette definition. We can assign continuous or discrete colors for the pixels based on their chlorophyll values.

For the better assignment of unique colors for the pixels within a range of chlorophyll values, we have considered the assignment in discrete fashion. For the purpose of generating the dataset for semantic segmentation, we have tailored the existing palettes and used them on the CHL_NN band images.

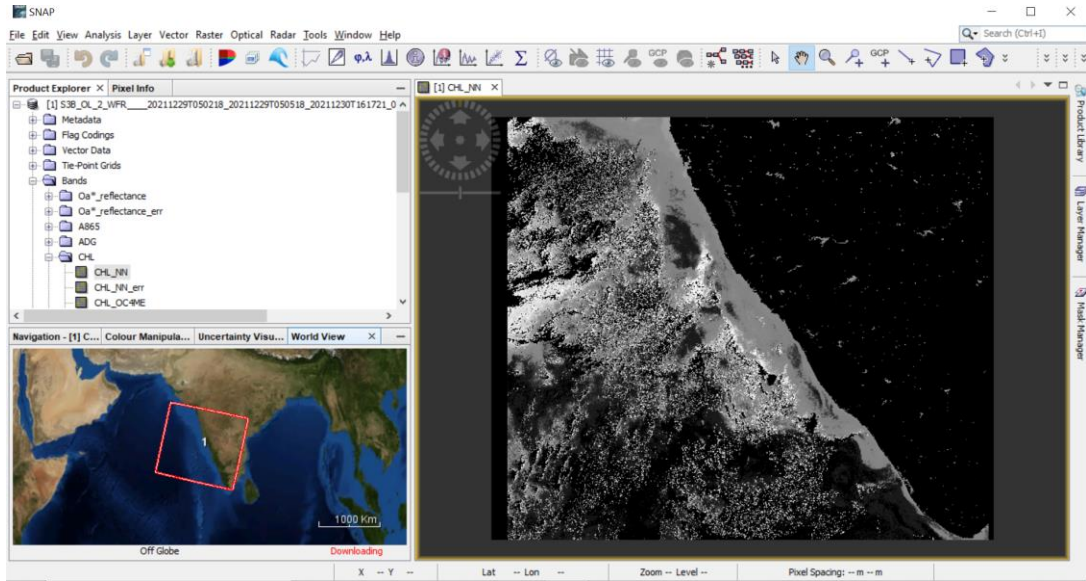


Fig. 2. Default grayscale image of the CHL_NN band present within satellite image captured on 29-12-2021

Tab. 2. Tailoring of existing gray_scale palette definition file in SNAP

| Default palette definition | | Tailored palette definition | |
|-------------------------------|--------------------------|-------------------------------|--------------------------|
| Chlorophyll (mg/m3) | Color assigned (R, G, B) | Chlorophyll (mg/m3) | Color assigned (R, G, B) |
| 0.0000001 | (0, 0, 0) | 0.0000001 to 0.2 | (102,102,102) |
| 0.2 | (51, 51, 51) | 0.2 to 1.8 | (153,153,153) |
| 0.4 | (102, 102, 102) | 1.8 to 8.0 | (204,204,204) |
| 0.6 | (153, 153, 153) | 8.0 to 42.9999997 | (255,255,255) |
| 0.8 | (204, 204, 204) | | |
| 1.0 | (255, 255, 255) | | |
| Number of points / colors = 6 | | Number of points / colors = 4 | |

This research is concentrated on grouping algal blooms into 3 major categories, namely, LOW BLOOM, MEDIUM BLOOM, and HIGH BLOOM. Along with this, the authors are considering the image area with significantly less amount of chlorophyll as the WATER part. The region in which there is no chlorophyll value is considered a background. This background represents the earth or land space, which has no chlorophyll content. This also represents the presence of clouds in the acquired images. Hence, there are 4 classes of image regions that are being considered in our research. To obtain the grayscale image with these 4 major classes of pixels, the authors have tailored the existing 'gray_scale' palette definition file as given in Tab. 2.

The R, G, and B color values of (0, 0, 0) are assigned to all the pixels that have the chlorophyll values within the range 0.0000001 to 0.1999999. The color values of (51, 51, 51) are assigned to all the pixels having chlorophyll values of range 0.2 to 0.3999999 and so on. Finally, all the pixels that have chlorophyll values from 1.0 and above are assigned color values of (255, 255, 255). Hence there are 6 color points in the default definition file. In the tailored palette definition file, the authors assigning the R, G, and B color values of (102, 102, 102) to the pixels with chlorophyll values within the range 0.2 to 1.7777779. The values (153, 153, 153) are assigned to pixels with a chlorophyll range of 1.8 to 7.9. The values (204,204,204) are assigned to pixels with a chlorophyll range of 8.0 to 42.8888889. The values (255, 255, 255) are assigned to all the pixels with chlorophyll values of 42.9999997 and above. Figure 3 shows the difference between images obtained with the default palette and tailored palette onto the CHL_NN band of the image captured on 29-12-2022.

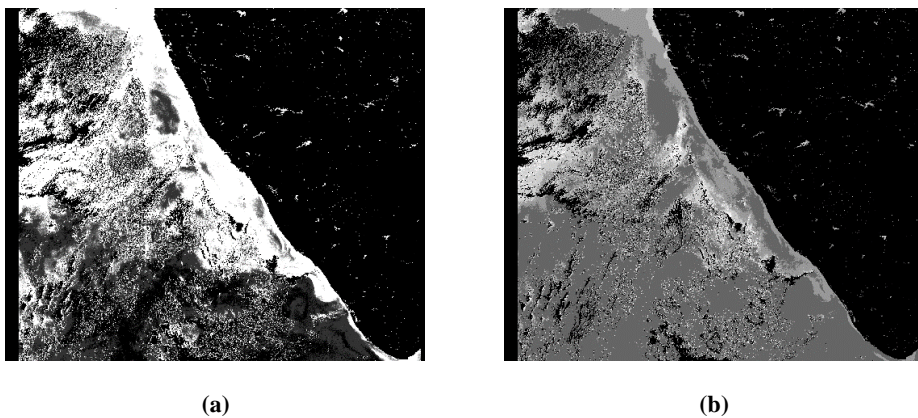


Fig. 3. Grayscale images obtained from CHL_NN band of satellite image captured on 29-12-2022 (a) Image obtained using default color palette definition file (b) Image obtained using tailored color palette definition file

To explore the presence of chlorophyll concentration in satellite images, SNAP provides a ‘cc_chl’ color palette. The default implementation of ‘cc_chl’ color palette has 8 different color definitions for assigning to different pixels based on their chlorophyll values. The authors have obtained the tailored definition file for this palette for adopting to our dataset. The default and tailored definitions of ‘cc_chl’ color palette is given in Tab. 3. The (R,G,B) combination of values (0,0,128) produces blue color and is used to signify the presence of water in the image. Values (0,153,51) produce green color and signify LOW BLOOM. Values (255, 255, 91) produce yellow color and signify MEDIUM BLOOM. Values (204,0,0) produce a red color and signify HIGH BLOOM. The default ‘gray_scale’ palette has 6 different color points, and the ‘cc_chl’ color palette has 8 different color points. These palettes are tailored to 4 different color points. During conversion in both cases, the corresponding range of chlorophyll values is maintained the same. Only the range of pixel values in the destination color points is changed. This ensures consistency in the obtained grayscale and color images.

Tab. 3. Definition of cc_chl color palette

| Default palette definition | | Tailored palette definition | |
|-------------------------------|--------------------------|-------------------------------|--------------------------|
| Chlorophyll Value (mg/m3) | Color assigned (R, G, B) | Chlorophyll Value (mg/m3) | Color assigned (R, G, B) |
| 0.1 | (0, 0, 128) | 0.0000001 to 0.2 | (0, 0, 128) |
| 0.3 | (51, 102, 255) | 0.2 to 1.8 | (0, 153, 51) |
| 1.0 | (0, 176, 220) | 1.8 to 8.0 | (255, 255, 91) |
| 2.5 | (0, 153, 51) | 8.0 to 42.9999997 | (204, 0, 0) |
| 5.0 | (255, 255, 91) | | |
| 10.0 | (230, 51, 0) | | |
| 25.0 | (204, 0, 0) | | |
| 59.9999997 | (128, 0, 0) | | |
| Number of points / colors = 8 | | Number of points / colors = 4 | |

Figure 4 shows the difference between images obtained after superimposing the default ‘cc_chl’ color palette and tailored ‘cc_chl’ palette. The figure depicts the CHL_NN band of the image captured on 29-12-2022. In Fig. 4(a), we can see eight different colors for eight different classes of algal bloom concentrations. Figure 4(b) depicts four colors for four classes of algal bloom concentrations considered in our research.

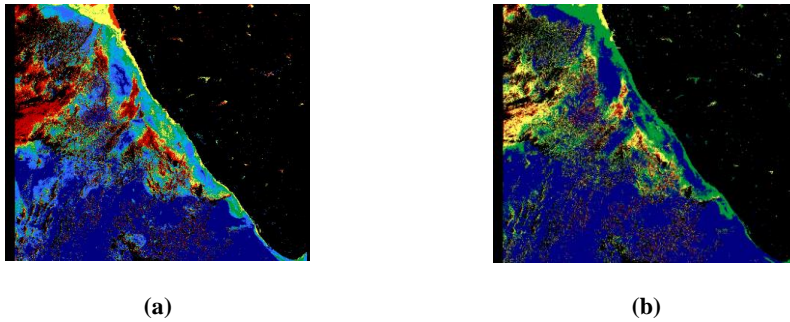


Fig. 4. Color images obtained from CHL_NN band after superimposing cc_chl color palette (a) Image obtained using default color palette definition file (b) Image obtained using tailored color palette definition file

These high-resolution CHL_NN bands having 4865 pixels of width and 4091 pixels of height are exported and saved in the form of an image. For the purpose of processing, these larger images are split into smaller images with dimensions of 256 pixels width and 256 pixels height. Each high-resolution image results in around 300 smaller images. Some of the produced images will have a black border or a single column of pixels. We have discarded such images manually. There is a future scope to develop deep learning models for semantic segmentation of algal blooms. Hence the size of 256x256 pixels is considered for the generation of images. The data set consists of a total of 5000 images. Figure 5 depicts some of the grayscale images and the corresponding color images with different bloom concentrations. Some of the images that were discarded from the dataset are depicted in Fig. 6.

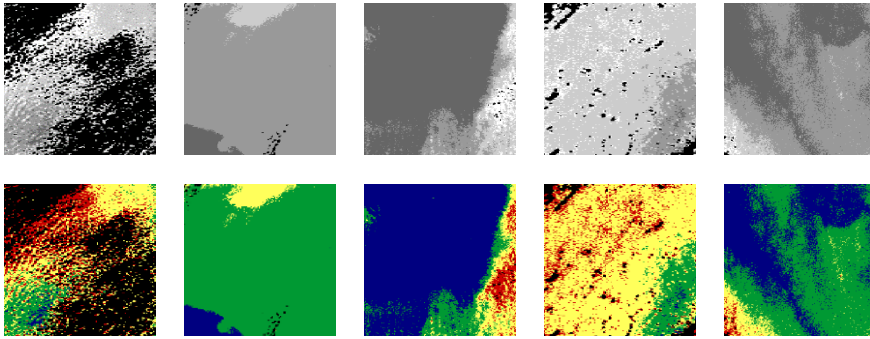


Fig. 5. Raw images considered in semantic segmentation of algal bloom concentrations and their corresponding ground truth images

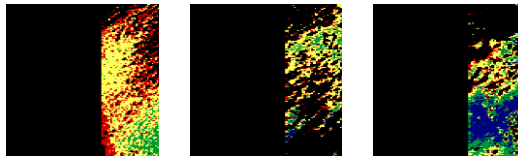


Fig. 6. Some of the images which were manually discarded from the dataset

The authors attempt to segment the images into 3 classes of blooms as **LOW**, **MEDIUM**, and **HIGH**. The increased volume of bloom, **HIGH** range, causes death of fish on the ocean surface. The **LOW** and **MEDIUM** quantities of bloom have minimal impact on fish or the environment. The research can be further extended to compare the impact of bloom concentration on aquatic life, such as the deaths of a large number of fish under the bloom. There is a scope to develop techniques for early detection of changes from **LOW** to **MEDIUM** concentration and **MEDIUM** to **HIGH** concentration. With this future motive, the authors have divided the bloom into 3 major classes.

4. RESULTS AND DISCUSSION

The authors automate the previously manual process of segmenting satellite images into different bloom concentrations. A rule-based classifier is developed for achieving semantic segmentation of image regions into **WATER**, **LOW**, **MEDIUM**, **HIGH**, and **BACKGROUND**.

4.1. Rule-based classification

To develop the rules, the presence of chlorophyll in the images is divided into different regions, five in this case. Appropriate grayscale values are assigned to represent this division. Then these grayscale images are mapped to corresponding color areas of blue, green, yellow, red, and black to represent different segmented regions. The procedure is depicted in Fig. 7. The algorithm for segmentation of bloom into different concentrations is presented in

Algorithm 1. The devised rules for the semantic segmentation of algal blooms into different regions are given in Tab. 4.

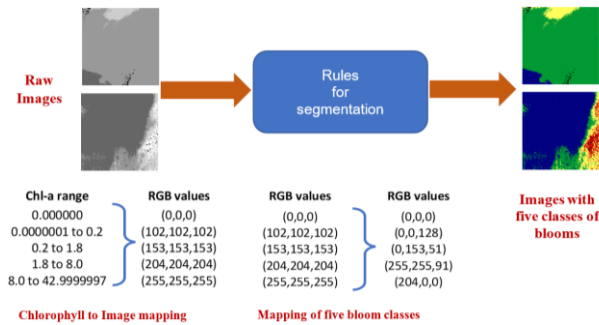


Fig. 7. Process of semantic segmentation of blooms

Tab. 4. Sample rules for semantic segmentation of bloom

| No. | Bloom level | Devised rule for segmentation |
|-----|-------------|---|
| 1 | Low | For every pixel in the image obtained using grayscale palette, IF (The pixel values of RGB channels are (153,153,153)) THEN label the corresponding pixel as GREEN |
| 2 | Medium | For every pixel in the image obtained using grayscale palette, IF (The pixel values of RGB channels are (204,204,204)) THEN label the corresponding pixel as YELLOW |
| 3 | High | For every pixel in the image obtained using grayscale palette, IF (The pixel values of RGB channels are (255,255,255)) THEN label the corresponding pixel as RED |
| 4 | Water | For every pixel in the image obtained using grayscale palette, IF (The pixel values of RGB channels are (102,102,102)) THEN label the corresponding pixel as BLUE |
| 5 | Background | For every pixel in the image obtained using grayscale palette, IF (The pixel values of RGB channels are (0,0,0)) THEN label the corresponding pixel as BLACK |

Algorithm 1: Semantic segmentation of algal bloom

Input: Raw satellite image of Indian ocean.

Output: Image segmented with low, medium and high algal bloom concentrations.

Process: The image will be scanned pixel-by-pixel from left to right and top to bottom. The RGB values of every pixel are compared with derived values. The pixels are categorized/segmented into blue, green, yellow, red and black regions indicating water, low bloom, medium bloom, high bloom and no bloom parts, respectively.

Begin

Step 1: Read the input image as IMAGE

Step 2: for (Each row present in the IMAGE) perform

Step 2.1: for (Each column present in the IMAGE) perform

Step 2.1.1: if RGB values of pixel at (row, column) equals to (0,0,0)
then assign RGB values of (0,0,0) to that pixel

Step 2.1.2: else-if RGB values of pixel at (row, column) equals to (102,102,102)

then assign RGB values of (0,0,128) to that pixel
 Step 2.1.3: else-if RGB values of pixel at (row, column) equals to (153,153,153)
 then assign RGB values of (0,153,51) to that pixel
 Step 2.1.4: else-if RGB values of pixel at (row, column) equals to (204,204,204)
 then assign RGB values of (255,255,91) to that pixel
 Step 2.1.5: else-if RGB values of pixel at (row, column) equals to (255,255,255)
 then assign RGB values of (204,0,0) to that pixel
 Step 3: Display the segmented IMAGE into five different classes
 End

4.2. Experimental results

The raw images in the dataset are input to the devised rule-based classifier. The rules were developed using a Python tool. The obtained results are validated by using the pixel-by-pixel comparison method. Some of the sample test images, segmented images, and their corresponding ground truth images are depicted in Fig. 8. To validate the obtained results, we have randomly selected 100 images obtained after applying rule-based semantic segmentation. The corresponding known ground truth images, images with known classes of blooms, for these 100 images are selected from our dataset. The pixel-by-pixel comparison is performed between these sampled groups of images.

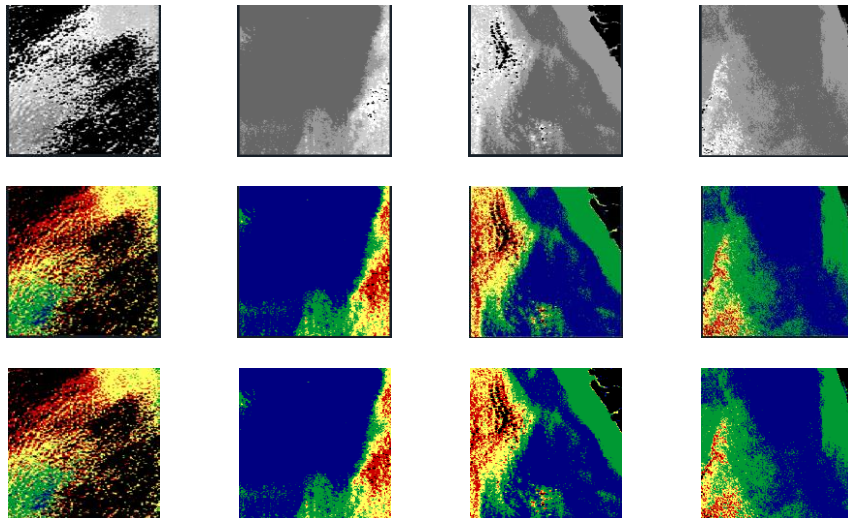


Fig. 8. Results of semantic segmentation of algal bloom concentrations. Every column depicts the sample test image, its segmented image, and its corresponding ground truth

An image is considered to be accurately segmented if all its pixels are properly assigned to their corresponding 4 bloom classes without any single pixel being wrongly assigned to a different class. If any of the pixels is wrongly assigned a different class, then it is not treated as segmented. A total of 98 images are properly being segmented into 4 bloom classes considered in our research. This experimentation of random selection of 100 images and the corresponding ground truth images is repeated an additional 4 times. The obtained results are tabulated, and the average result of all 5 experiments is claimed as the accuracy of the

developed rule-based classifier. The results are given in Tab. 5. The average accuracy of semantic segmentation obtained using a rule-based classifier is 98%.

Tab. 5. Results of semantic segmentation

| Experiment No. | 1 | 2 | 3 | 4 | 5 |
|-----------------------------|----|----|----|----|----|
| Accurately Segmented images | 98 | 97 | 99 | 98 | 98 |

The predicted algal blooms can be measured with in-situ data. The bloom samples can be physically collected from the region being analyzed. The chlorophyll content of the collected sample can be manually estimated in the laboratory setup. The laboratory results and algorithm results can be compared. The process is laborious, costly, and time-consuming. As we have not validated the results using in-situ data, we used the manual validation approach in the SNAP tool. The area being segmented is selected with the mouse, and chlorophyll content in that region is examined. The chlorophyll value is compared with the segmented class of bloom based on color. We have followed manual validation as in-situ validation was not feasible under the research circumstances.

4.3. Comparative study

Different research has been conducted on algal bloom segmentation. A rule-based approach for semantic segmentation of algal blooms has not been attempted by earlier researchers.

Tab. 6. Comparison of our work with existing works

| Reference | Work carried out | Dataset used | Technique | Accuracy (%) |
|----------------------------------|---|-----------------------------------|---|--------------|
| (Fernández-Tejedor et al., 2022) | Estimation of Chl-a concentration | Sentinel-2 images | Generated chlorophyll maps using the SNAP tool. | 70.00 |
| (Cui et al., 2022) | Semantic segmentation of green tide | MODIS | Presented a super-resolution-based segmentation network | 96.88 |
| (Singh et al., 2023) | Semantic segmentation of satellite images | Drone multispectral data | Deep learning is adopted for semantic segmentation. | 90.60 |
| (Ioannis & Maria, 2022) | Semantic segmentation of satellite images | Sentinel-2 images | A deep learning approach is utilized. | 90.00 |
| (Lilay & Taye, 2023) | Land cover classification from satellite images | Sentinel-2 satellite images | LinkNet model is used. | 88.20 |
| (Radhika et al., 2022) | Semantic segmentation of paddy crops and weeds | Dataset created by digital camera | PSPNet and UNet | 90.00 |
| Our work | Semantic segmentation of algal blooms | Sentinel 3A/3B | Rule-based approach | 98.00 |

The comparison of the work is made with some of the other relevant works as given in Tab. 6. From the comparative study, it is evident that the proposed rule-based technique has produced better accuracy in segmentation.

5. CONCLUSIONS

Algal blooms (ABs) are considered to be harmful when they grow beyond the acceptable level on the sea surface. They may cause harmful effects on aquatic life and may affect the economy. Satellite imagery plays a significant role in tracking the growth of algal blooms. Sentinel 3A/3B images are considered in this research. The band containing the details of chlorophyll-a, chl_nn, from sentinel products is utilized in this study. The dataset is created by using Chl_nn band images. The semantic segmentation technique is adopted in classifying algal bloom regions into low, medium, and high concentrations. A rule-based classifier is developed that utilizes the gray level values corresponding to the level of bloom concentration present in the region. The rules segment the image into the water part, low-level bloom, medium-level bloom, high-level bloom, and background. The developed rule-based segmentation technique has produced an average accuracy of 98%. The proposed methodology demonstrates that semantic segmentation can be adopted in an algal bloom study. The proposed dataset can be used for training deep learning classifiers, such as U-NET, FCN, and Deeplab. The rule-based segmentation technique can be effectively utilized in the semantic segmentation of algal blooms. The methodology finds applications in developing a system to monitor the excess growth of algal blooms and to prevent their hazardous impact on aquatic life.

Author contributions

Venkatesh BHANDAGE: Data curation, Methodology, Writing-Original draft preparation, Software, Validation. Manohara PAI M. M.: Conceptualization, Supervision, Writing-Reviewing and Editing.

Funding

This research has received no funds.

Acknowledgments

Authors would like to thank European Organisation for the Exploitation of Meteorological Satellites (EUMETSAT) for making the required satellite images available.

Conflicts of Interest

The authors declare that there are no conflicting interests.

Data availability

The data that support the findings of this study are available from the corresponding author upon reasonable request.

REFERENCES

- Al-Nawashi, M. M., Al-Hazaimeh, O. M., & Khazaaleh, M. Kh. (2024). New approach for breast cancer detection based on machine learning techniques. *Applied Computer Science*, 20(1), 1-16. <https://doi.org/10.35784/acs-2024-01>
- Anilkumar, P., & Venugopal, P. (2022). Research contribution and comprehensive review towards the semantic segmentation of aerial images using Deep Learning techniques. *Security and Communication Networks*, 2022(1), 6010912. <https://doi.org/10.1155/2022/6010912>
- Badrinarayanan, V., Kendall, A., & Cipolla, R. (2017). SegNet: A deep convolutional encoder-decoder architecture for image segmentation. *IEEE Transactions on Pattern Analysis and Machine Intelligence*, 39(12), 2481-2495. <https://doi.org/10.1109/TPAMI.2016.2644615>
- Baran, K. (2024). Application of thermal imaging cameras for smartphone: Seek Thermal Compact Pro and FLIR One Pro for human stress detection – Comparison and study. *Applied Computer Science*, 20(1), 122–138. <https://doi.org/10.35784/acs-2024-08>
- Cui, B., Zhang, H., Jing, W., Liu, H., and Cui, J. (2022). SRSe-Net: Super-Resolution-Based semantic segmentation network for green tide extraction. *Remote Sensing*, 14(3), 710. <https://doi.org/10.3390/rs14030710>
- Elbahri, M., Taleb, N., Ardjoun, S. A. E. M., & Zouaoui, C. M. A. (2024). Few-shot learning with pre-trained layers integration applied to hand gesture recognition for disabled people. *Applied Computer Science*, 20(2), 1-23. <https://doi.org/10.35784/acs-2024-13>
- EUMETSAT. (2024). *OLCI Level-2 Water Full Resolution*. <http://codata.eumetsat.int/#/home>
- Fernández-Tejedor, M., Velasco, J. E., & Angelats, E. (2022). Accurate estimation of chlorophyll-a concentration in the coastal areas of the ebro delta (NW Mediterranean) using Sentinel-2 and its application in the selection of areas for mussel aquaculture. *Remote Sensing*, 14(20), 5235. <https://doi.org/10.3390/rs14205235>
- Fogg, G. E. (2022). Harmful algae - A perspective. *Harmful Algae*, 1(1), 1-4. [https://doi.org/10.1016/S1568-9883\(02\)00002-1](https://doi.org/10.1016/S1568-9883(02)00002-1)
- Girisha, S., Pai, M. M. M., Verma, U., & Pai, R. M. (2021a). Semantic segmentation with enhanced temporal smoothness using CRF in aerial videos. *IEEE Madras Section Conference (MASCONE)* (pp. 1-5). IEEE. <https://doi.org/10.1109/MASCONE51689.2021.9563599>
- Girisha, S., Verma, U., Manohara Pai, M. M., & Pai, R. M. (2021b). UVID-Net: Enhanced semantic segmentation of UAV aerial videos by embedding temporal information. *IEEE Journal of Selected Topics in Applied Earth Observations and Remote Sensing*, 14, 4115-4127. <https://doi.org/10.1109/JSTARS.2021.3069909>
- Haji Gholizadeh, M., Melesse, A. M., & Reddi, L. (2016). Spaceborne and airborne sensors in water quality assessment. *International Journal of Remote Sensing*, 37(14), 3143-3180. <https://doi.org/10.1080/01431161.2016.1190477>
- Ho, J. C., Michalak, A. M., & Pahlevan, N. (2019). Widespread global increase in intense lake phytoplankton blooms since the 1980s. *Nature*, 574, 667-670. <https://doi.org/10.1038/s41586-019-1648-7>
- Jaiganesh, S. N. N., Sarangi, R. K., & Shukla, S. (2021). Satellite-based observation of ocean productivity in southeast Arabian Sea using chlorophyll, sea surface temperature and wind datasets. *Journal of Earth System Science*, 130, 5. <https://doi.org/10.1007/s12040-020-01512-y>
- Kamath, R., Balachandra, M., Vardhan, A., & Maheshwari, U. (2022). Classification of paddy crop and weeds using semantic segmentation. *Cogent Engineering*, 9(1), 2018791. <https://doi.org/10.1080/23311916.2021.2018791>
- Kinane Daouadji, A., & Bendella, F. (2024). Improving e-learning by facial expression analysis. *Applied Computer Science*, 20(2), 126-137. <https://doi.org/10.35784/acs-2024-20>
- Kotaridis, I., & Lazaridou, M. (2022). Semantic segmentation using a UNet architecture on Sentinel-2 data. *The International Archives of the Photogrammetry, Remote Sensing and Spatial Information Sciences, XLIII-B3-2022*, 119-126. <https://doi.org/10.5194/isprs-archives-XLIII-B3-2022-119-2022>
- Kutser, T. (2009). Passive optical remote sensing of cyanobacteria and other Intense phytoplankton blooms in coastal and inland waters. *International Journal of Remote Sensing*, 30(17), 4401-4425. <https://doi.org/10.1080/01431160802562305>

- Li, Z., & Demir, I. (2023). U-net-based semantic classification for flood extent extraction using SAR imagery and GEE platform: A case study for 2019 central US flooding. *Science of the Total Environment*, 869, 161757. <https://doi.org/10.1016/j.scitotenv.2023.161757>
- Lilay, M. Y., & Taye, G. D. (2023). Semantic segmentation model for land cover classification from satellite images in Gambella National Park, Ethiopia. *SN Applied Sciences*, 5, 76. <https://doi.org/10.1007/s42452-023-05280-4>
- Ma, J., Zhou, W., Lei, J., & Yu, L. (2023). Adjacent bi-hierarchical network for scene parsing of remote sensing images. *IEEE Geoscience and Remote Sensing Letters*, 20, 3000705. <https://doi.org/10.1109/LGRS.2023.3241648>
- Maiyanti, S. I., Desiani, A., Lamin, S., Puspitashati., Arhami, M., Gofar, N., & Cahyana, D. (2023) Rotation-gamma correction augmentation on CNN-dense block for soil image classification. *Applied Computer Science*, 19(3), 96-115. <https://doi.org/10.35784/acs-2023-27>
- Makhlouf, Z., Meraoumia, A., Lakhdar, L., & Haouam, M. Y. (2024). Enhancing medical data security in e-health systems using biometric-based watermarking. *Applied Computer Science*, 20(1), 28-55. <https://doi.org/10.35784/acs-2024-03>
- Nallapareddy, A., (2022). Detection and classification of vegetation areas from red and near infrared bands of Landsat-8 optical satellite image. *Applied Computer Science*, 18(1), 45-55. <https://doi.org/10.35784/acs-2022-4>
- Nayak, R. K., Swapna, M., Manche, S. S., Mohanty, P. C., Sheshasai, M. V. R., Dadhwal, V. K., & Kumar, R. (2023). Assessment of chlorophyll-a seasonal cycle in the North Indian Ocean using observations from OCM2, MODIS, and SeaWiFS. *Journal of the Indian Society of Remote Sensing*, 51, 229-246. <https://doi.org/10.1007/s12524-022-01642-4>
- Ogashawara, I. (2019). The use of Sentinel-3 imagery to monitor cyanobacterial blooms. *Environments*, 6(6), 60. <https://doi.org/10.3390/environments6060060>
- Randolph, K., Wilson, J., Tedesco, L., Li, L., Pascual, D. L., & Soyeux, E. (2008) Hyperspectral remote sensing of cyanobacteria in turbid productive water using optically active pigments, chlorophyll a and phycocyanin. *Remote Sensing of Environment*, 112(11), 4009-4019. <https://doi.org/10.1016/j.rse.2008.06.002>
- Ravishankar, T., Anil, T. C., Verma, U., Pai, M. M. M., & Pai. R. (2022). MartiNet: An efficient approach for river segmentation in SAR images. *IEEE International Conference on Electronics, Computing and Communication Technologies (CONECCT)* (pp. 1-6). IEEE. <https://doi.org/10.1109/CONECCT55679.2022.9865830>
- Rodríguez-Benito, C. V., Navarro, G., & Caballero, I. (2020). Using Copernicus Sentinel-2 and Sentinel-3 data to monitor harmful algal blooms in Southern Chile during the COVID-19 lockdown. *Marine Pollution Bulletin*, 161(Part A), 111722. <https://doi.org/10.1016/j.marpolbul.2020.111722>
- Roelke, D., & Buyukates, Y. (2001). The Diversity of harmful algal bloom-triggering mechanisms and the complexity of bloom initiation. *Human and Ecological Risk Assessment: An International Journal*, 7(5), 1347-1362. <https://doi.org/10.1080/20018091095041>
- Ronneberger, O., Fischer, P., & Brox, T. (2015). U-Net: Convolutional Networks for Biomedical Image Segmentation. In N. Navab, J. Hornegger, W. M. Wells, & A. F. Frangi (Eds.), *Medical Image Computing and Computer-Assisted Intervention – MICCAI 2015* (Vol. 9351, pp. 234–241). Springer International Publishing. https://doi.org/10.1007/978-3-319-24574-4_28
- Shelhamer, E., Long, J., & Darrell, T. (2017). Fully convolutional networks for semantic segmentation. *IEEE Transactions on Pattern Analysis and Machine Intelligence*, 39(4), 640-651. <https://doi.org/10.1109/TPAMI.2016.2572683>
- Singh, N. J., & Nongmeikapam, K. (2023). Semantic segmentation of satellite images using Deep-Unet. *Arabian Journal for Science and Engineering*, 48, 1193–1205. <https://doi.org/10.1007/s13369-022-06734-4>
- Srichandan, S., Baliarsingh, S. K., Samanta, A. Jena, A. K., Lotliker, A. A., Nair, T. M. B., Barik, K. K., & Acharyya, T. (2022). Satellite-based characterization of phytoplankton blooms in coastal waters of the northwestern bay of bengal. *Journal of the Indian Society of Remote Sensing*, 50, 2221-2228. <https://doi.org/10.1007/s12524-022-01597-6>
- Tendolkar, A., Choraria, M. M., Manohara Pai, S., Girisha, G., Dsouza & Adithya, K. S. (2021). Modified crop health monitoring and pesticide spraying system using NDVI and Semantic Segmentation: An AGROCOPTER based approach. *IEEE International Conference on Autonomous Systems (ICAS)* (pp. 1-5). IEEE. <https://doi.org/10.1109/ICAS49788.2021.9551116>
- Tholkapiyan, M., Shanmugam, P., & Suresh, T. (2014). Monitoring of ocean surface algal blooms in coastal and oceanic waters around India. *Environmental Monitoring and Assessment*, 186, 4129–4137. <https://doi.org/10.1007/s10661-014-3685-x>

- Vase, V. K., Ajay, N., Kumar, R. Jayaraman, J., & Rohit, P. (2022). Evaluation of satellite sensors to compute Chlorophyll-a concentration in the Northeastern Arabian Sea: A validation approach. *Journal of the Indian Society of Remote Sensing*, 50, 2209-2220. <https://doi.org/10.1007/s12524-022-01598-5>
- Verma, U., Chauhan, A., Manohara, M.P., & Pai, R. (2021). DeepRivWidth: Deep Learning based semantic segmentation approach for river identification and width measurement in SAR images of coastal Karnataka. *Computers & Geosciences*, 154, 104805. <https://doi.org/10.1016/j.cageo.2021.104805>
- Wang, Z., Zhang, S., Zhang, C., & Wang, B. (2023). Hidden feature-guided semantic segmentation network for remote sensing images. *IEEE Transactions on Geoscience and Remote Sensing*, 61, 1-17, 5603417. <https://doi.org/10.1109/TGRS.2023.3244273>
- Yang, N., & Tang, H. (2021). Semantic segmentation of satellite images: A Deep Learning approach integrated with geospatial hash codes. *Remote Sensing*, 13(14), 2723. <https://doi.org/10.3390/rs13142723>
- Zhu, S., Wu, Y., & Ma, X. (2023). Deep Learning-based algal bloom identification method from remote sensing images - Take China's Chaohu Lake as an example. *Sustainability*, 15(5), 4545. <https://doi.org/10.3390/su15054545>